Jornadas de Automática

Advancements in the modeling of IH-DTL cavities for control applications

Beñat González[a,*], Iñigo Arredondo[a], Joaquín Portilla[a], Markel Larrea[a], Jorge Feuchtwanger[a,b], Andoni Egurrola[c]

[a]*Department of Electricity and Electronics (EHU), Unibersitateko Errepidea 2, 48940 Santsoena, Bizkaia.*
[b]*Ikerbasque, Basque Foundation for Science, 48009 Bilbao, Spain.*
[c]*Tekniker, Parke Teknologikoa Iñaki Goenaga 5, 20600 Eibar. Gipuzkoa*

To cite this article: González, B., Arredondo, I., Portilla, J., Larrea, M., Feuchtwanger, J., Egurrola, A. 2026. Advancements in the modeling of an IH-DTL cavity for control applications.
Jornadas de Automática, 47. https://doi.org/10.17979/ja-cea.2026.47.13744

Resumen

El control activo de cavidades resonantes es esencial para optimizar el rendimiento de los aceleradores de partículas. Esto requiere un modelado preciso que caracterice la respuesta de la cavidad frente a diversos parámetros controlables. Una arquitectura compacta y eficiente para la aceleración de energías bajas-medias es el *Interdigital H-Mode Drift Tube Linac* (IH-DTL). Sin embargo, la literatura actual carece de modelos adecuados para simulaciones orientadas al control debido a que los enfoques estándar tratan la cavidad como una entidad monolítica. Esto impide el modelado de efectos posicionales cruciales, como el sintonizado (tuning) localizado. Este trabajo presenta una metodología para caracterizar cada sección de aceleración individual como parte de un circuito a parametros concentrados y se valida utilizando una estructura IH-DTL real. Basándonos en esta discretización, presentamos un circuito equivalente distribuido diseñado para capturar dependencias espaciales localizadas. Esta representación de parámetros concentrados es particularmente ventajosa, ya que facilita su integración y simulación dentro de entornos de computación estándar.

Palabras clave: Identificación para control, Validación de Modelo, Modelo de caja gris, Sistemas de parámetros concentrados, Aplicaciones de control

Abstract

Active control of resonant cavities is essential for optimizing particle accelerator performance. This requires accurate modeling to characterize cavity responses to various controllable parameters. A compact and efficient architecture for low-to-medium energy acceleration is the *Interdigital H-Mode Drift Tube Linac* (IH-DTL). However, current literature lacks models suitable for control-oriented simulations because standard approaches treat the cavity as a monolithic entity. This prevents the modeling of crucial positional effects, such as localized tuning. This work introduces a methodology to characterize individual accelerating sections as standard electrical components and validates it by applying it to an actual IH-DTL structure. Building upon this discretization, we present a novel distributed equivalent circuit designed to capture localized spatial dependencies. This lumped-element representation is particularly advantageous, as it enables seamless integration and simulation within standard computational frameworks used in control engineering.

Keywords: Identification for control, Model validation, Grey box modeling, Lumped-parameter models, Control applications

1. Introduction

Active control of resonant cavities is essential for optimizing performance and maintaining beam stability in particle accelerators. The implementation of effective control systems requires accurate modeling to characterize how the cavity responds to various controllable parameters. For low-to-medium energy applications, the Interdigital H-Mode Drift Tube Linac (IH-DTL) is a compact and efficient architecture. However, while current literature provides models for the gen-

*Corresponding author: benat.gonzalez@ehu.eus

eral design of these cavities, there is a lack of models suitable for control-oriented simulations.

Historically, the design and analysis of IH-DTL cavities have relied on the analytical model presented by Ratzinger (2005). This approach is widely used in the literature concerning IH-DTL structures (Lu et al., 2007; Tan et al., 2018) and provides a reliable basis for understanding general cavity behavior and selecting initial design parameters. While treating the cavity as a single entity is practical for initial design, such global models are insufficient for control purposes. In practice, the Low-Level Radio Frequency (LLRF) control scheme relies on physical tuners whose influence on the system varies significantly depending on their spatial position. Consequently, a distributed model is necessary to capture these position-dependent behaviors and accurately represent the mechanisms that the control actuators must influence.

The objective of this work is to study methods for discretizing the cavity to better understand localized effects such as the impact of individual tuners, various injection mechanisms, manufacturing tolerances, and environmental disturbances such as microphonics or thermal shifts. All these detailed phenomena are not captured by any existing global analytical models, but are essential for designing precise tuning and control systems. In this paper, we present a methodology to characterize the individual accelerating sections of the cavity and show the advances made on a novel distributed equivalent circuit designed to capture positional effects. Representing the system as a lumped-element equivalent circuit is advantageous because it allows for simulation within standard computational frameworks used in control engineering. The method is applied to the IH-DTL cold model of the LINAC-7 project (Feuchtwanger et al., 2022), currently under development at the University of the Basque Country (UPV/EHU).

2. IH-DTL cavity

2.1. Working principle

Unlike conventional LINAC (LINear ACcelerator) structures that utilize TM modes with intrinsic longitudinal electric field components, the IH-DTL cavity generates an axial accelerating field through a sophisticated geometric configuration (see Fig. 1). Based on the TE_{111} mode, the cavity features a transverse magnetic field that circulates around the structure. By introducing stems, this magnetic field is forced to curl around the supports, inducing currents that charge the drift tubes. Since successive stems are connected to opposite sides of the cavity, alternating tubes accumulate opposing charges, thereby establishing the required longitudinal accelerating field along the axis.

In this way, we can separate the cavity in two different regions: the accelerating region, where the electric field is dominant and responsible for the acceleration of the particles, and the outer TE resonator region, where the magnetic field is dominant and responsible for coupling the different accelerating cells. This separation is crucial for understanding the working principle of the cavity and will be essential for the proposed equivalent circuit (Section 5).

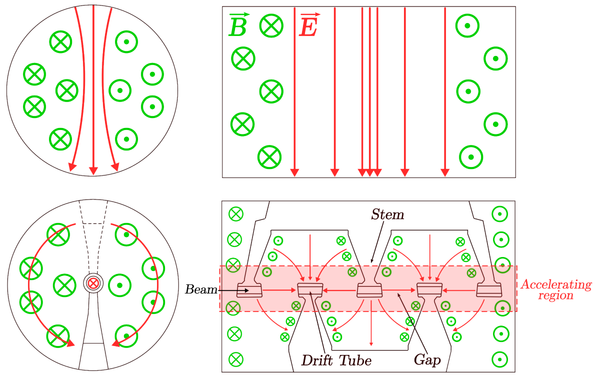

Figure 1: Scheme of the fields in a TE_{111} mode (top) show the field distribution on a cylindrical cavity without stems and drift tubes. When modified, $TE_{11(0)}$ (bottom), fields for axial acceleration appear, but the general shape of the fields in the outer part of the cavity remains largely unchanged.

2.2. Standard Equivalent circuit of the IH-DTL

The standard analytical model for the IH-DTL cavity is derived from the lumped-element equivalent circuit shown in Fig. 2. The electric capacitance per unit length of the accelerating region is represented by C'_D, which is determined analytically using the formulation for a cylindrical conductor shielded by two parallel planes. The external volume is modeled as a pair of parallel LC circuits. These lumped parameters are derived from Maxwell's equations (specifically through the electromagnetic energy stored within the resonant mode) under the resonance condition defined by $\omega = 1/\sqrt{LC}$.

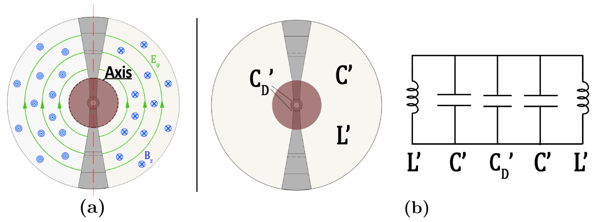

Figure 2: (a) Schematic of the fields on a transversal cut of the IH-DTL cavity and (b) the equivalent circuit proposed in the analytical model.

2.3. Control perspective

The primary objective of resonance control in these cavities is to synchronize the electromagnetic field with the particle beam to maximize energy transfer. To achieve this, the Low-Level Radio Frequency (LLRF) control system must ensure that the amplitude and phase of the RF drive signal remain synchronized with the requirements of the synchronous particle. Furthermore, the system must actively maintain the cavity's resonant frequency against external perturbations to match the operating frequency of the beam.

In practice, the control system operates through two primary sets of actuators: the RF drive signal (which modulates the amplitude and phase of the input via the power coupler) and mechanical tuners. These tuners consist of cylindrical plungers whose depth of insertion modifies the internal geometry of the cavity, thereby shifting its resonant frequency. As illustrated in Fig. 3, these tuners are distributed at various longitudinal positions along the cavity. To close the control loop, the generated electromagnetic field is monitored using a pick-up probe (RF sensor).

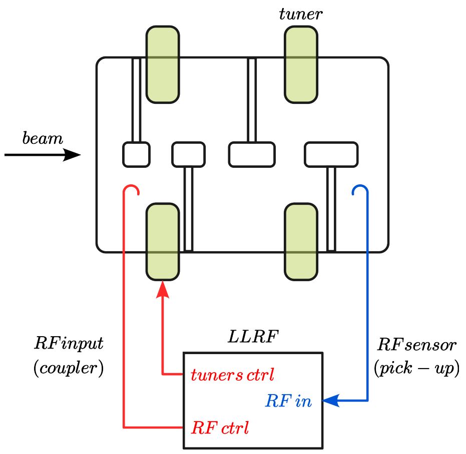

Figure 3: Schematic of the LLRF control.

The standard analytical model cannot account for the localized effects of these actuators, as their reactive contribution depends heavily on their spatial placement; a point further detailed in Section 4.4. Consequently, a discretized modeling approach is essential to accurately characterize the system's sensitivity to individual tuner adjustments.

3. Proposed equivalent circuit for control applications

The proposed equivalent circuit is illustrated in Fig. 4. As opposed to other DTLs, we can not rely on commonly used propagating wave models like the one presented by Jia and Zheng (2013). In this H-mode cavity, the mechanism unifying each section is the outer TE mode (TE resonator section in Fig. 4). Each resonant cell is represented by a parallel *RLC* network, while the inter-cell coupling is characterized by mutual inductances $M_{i,j} = k_{i,j}\sqrt{L_i L_j}$. These represent the magnetic field that ties all the cavity together. Defining the voltage in each resonant cell i as $V_i = q_i/C_i$, where q_i is the charge on each capacitor and the dot represents time derivatives, Kirchhoff's voltage law gives:

$$\left(L_i + \sum_{j\neq i} M_{ij}\right)\ddot{q}_i + R_i\dot{q}_i + \frac{q_i}{C_i} = 0 \qquad (1)$$

As the quality factor (Q) of the cavity is large, we can start by neglecting the damping term related to R_i. For steady state solutions like $q_i(t) = q_i e^{j\omega t}$; $\ddot{q}_i = -\omega^2 q_i$ we can get to

$$\underbrace{\mathbf{L}^{-1}\mathbf{C}^{-1}}_{\mathbf{A}}\ \mathbf{q} = \omega^2\mathbf{q} \qquad (2)$$

where the parameters in bold represent the vectors of charges and matrices of inductances and capacitances.

This is a typical eigenvalue problem from which the resonant modes and voltage distribution can be obtained. The coupling coefficients $k_{i,j}$ and the parameters of each cell can be adjusted to match the $TE_{11(0)}$ mode of the cavity. The resonant section of the cavity is conceptually divided into two sides corresponding to the two halves of the cavity.

On the other hand, the accelerating field for the particles is represented by the acceleration section in Fig. 4. The axial electric field is generated on the gap capacitors (C_{di}) and model the regions between drift tubes. The stem inductances (L_{si}) connect this capacitive elements to the main *RLC* cavity stages. By connecting each element to one of the cavities interdigitally, the π resonance mode (characterized by a 180° phase shift between adjacent gaps) emerges naturally as the fundamental operating mode of the system.

This circuit could allow the modeling of distributed effects from a control perspective. However, in order to validate the model and better understand the behavior of the cavity, a good characterization of the system must be performed first.

4. Characterization of lumped parameters in CST

Electromagnetic solvers like CST (Dassault Systèmes, 2024) provide a complete map of the field and energy distribution within the cavity. Using this information, it is possible to extract the lumped parameters of an equivalent RLC circuit via (3)(Grespan et al., 2010):

$$W_m = \frac{1}{2}L\,|I|^2 \qquad W_e = \frac{1}{2}C\,|V|^2 \qquad (3)$$

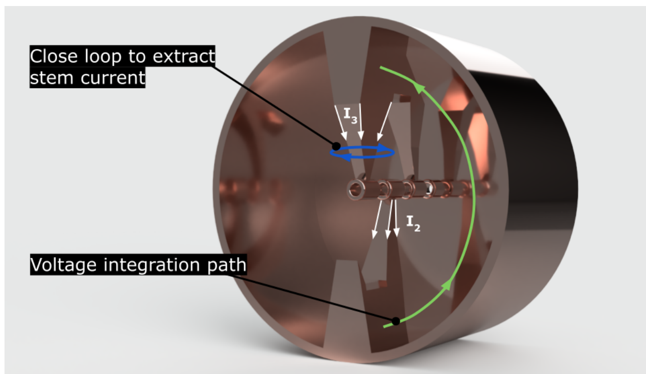

Figure 5: Dissected view of an IH-DTL cavity showing the first three accelerating sections. The integration paths to obtain currents and voltage differences are indicated.

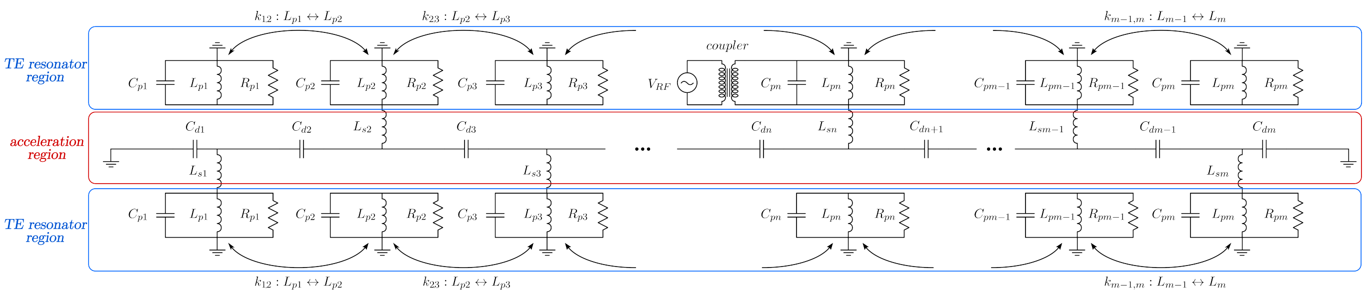

Figure 4: Proposed equivalent circuit.

where W_m and W_e represent the stored magnetic and electric energies in a given region and I and V are the current and voltage related to the lumped element to be extracted. For this reason, it is essential to identify how each specific region affects the field shape and the way energy is distributed throughout the structure in order to correctly characterize the different elements.

4.1. Characterization of the inductances

To determine the inductances of the system, we must first characterize the currents flowing through the cavity. We expect the current flowing out of the top stems to be equal to the current entering the bottom stems. These currents were quantified using Ampère's law by integrating the magnetic field over a closed loop near each stem, as shown in Fig. 5. Although the results are slightly sensitive to the specific integration path, the sum of the top and bottom currents shows a high degree of correlation, with over 95 % agreement. Furthermore, we assume that the current flowing through the cavity walls connects the two nearest stems to close the circuit.

Based on the working principle of the IH-DTL cavity, the inductance characterization is divided into two primary regions: the stems and the outer cavity. The stems serve as the connection between each side of the cavity and the differentially charged drift tubes. We denote the inductance associated with these stems as L_s, which is calculated using the individual stem currents and the magnetic energy stored around the stem. In contrast, the currents flowing along the cavity walls are associated with the parameter L_p, representing the inductance of the resonant mode. This value is determined by the magnetic energy stored in each cavity section, excluding the energy already accounted for within the stem regions. In this way:

$$L_s = \frac{2W_{m,s}}{|I|^2} \qquad L_p = \frac{2(W_m - W_{m,s})}{|I/2|^2} \tag{4}$$

where $W_{m,s}$ is the magnetic energy stored around the stem, W_m is the magnetic energy density integrated in the section volume and I is the current flowing through each stem. For L_p we have divided the current by 2 because the current flowing through each wall is half of that flowing through the stem.

4.2. Characterization of the capacitances

Following the same logic used for the inductances, the capacitances are divided into two regions: the center of the cavity, which contains over 70 % of the total electric energy, and the outer section, characterized by a transverse E-field that retains the shape of the original TE mode. The capacitance associated with the drift tubes, C_D, is calculated using the voltage difference between adjacent tubes and the energy stored along the axis in each section.

In contrast, the capacitance of the outer cavity region, C_p, is harder to determine because the results are highly sensitive to the choice of the integration path. To obtain the most reliable estimate, we selected the path corresponding to the part where the TE mode has been observed to dominate by looking at the energy distribution. The voltage calculated in paths around this radius is observed to be very similar.

4.3. Characterization of the resistances

As a first approach, the cavities are expected to work like resonators in parallel. To get R_p, then, each section should get N times the total cavity resistance. One approach to get the values of the resistances is to use the quality factor of the cavity, which can be obtained directly from CST or by S-parameter measurements (Ginzton, 1957). This leads to the total resistivity of the cavity, given by $Q = \omega_0 CR$ (Wangler, 2008).

4.4. Characterization of the tuner effects

One of the main effects we want to capture with the proposed model is the effect of the tuners. As mentioned before, these devices are cylindrical plungers that modify the geometry of the cavity and therefore its resonant frequency. To characterize their effect, we have simulated the cavity with different tuner positions and insertion depths. The results in Section 5 show that the tuners change the resonant frequency of the cavity linearly with the insertion depth, and that the slope of this change depends on the position of the tuner. In fact, the rate of change is related to that of the magnetic energy, which is highest in the center and lowers towards the ends of the cavity. The effect of the tuners can be included in the equivalent circuit by varying the inductor associated with the outer part of the cavity.

5. Application to the LINAC-7 cold model

To validate the proposed method, it was applied to the IH-DTL cold model of the LINAC-7 project. This cavity is designed as the final acceleration stage to increase a proton beam's energy from $3\,MeV$ to $7\,MeV$, and has an operating frequency of 750 MHz. It is currently being manufactured as part of a collaboration between the Tekniker technology center, the company Egile, the Ineustar association and the University of the Basque Country (UPV/EHU). The cavity consists of twelve gaps; consequently, the proposed method allows for the extraction of eleven distinct sets of parameters, one for each section (see Fig. 6 (b)).

Table 1: Comparison of analytical and CST-retrieved parameters for the 750MHz IH-DTL cavity of the LINAC-7 project.

Param.	**Analytical**	**One section (L=21.05mm)**	**Obtained from CST**
Cd	7.1738 pF/m	0.151 pF	0.124 - 0.136 pF
Cp	5.7358 pF/m	0.1207 pF	0.117 - 0.145 pF
Lp	4.4413 nHm	210.98 nH	44.6 - 50.2 nH

The results obtained from the proposed method and those derived from the analytical model are presented in Table 1. The analytical results are applied to a cavity with the average section length of the cold model. As shown, there is good agreement between the results for the capacitances, but the resonator inductances are considerably lower when extracted from the electromagnetic simulations. This means that each resonator alone should have a higher resonant frequency than the one of the whole cavity, which is consistent with the fact that the coupling between resonators is not negligible and that it lowers the resonant frequency of the system. This proves that the proposed approach is valid, even if it is not possible to completely relate the new circuit model with the simple analytical model used for design.

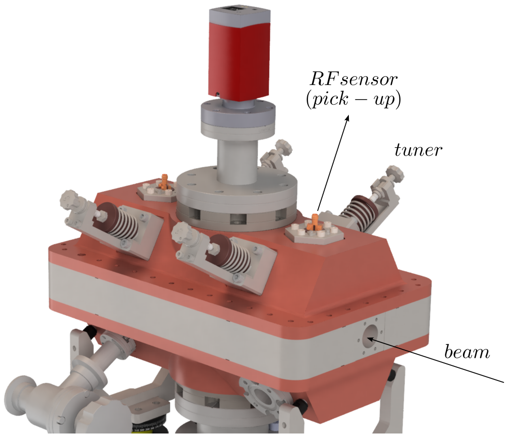

(a)

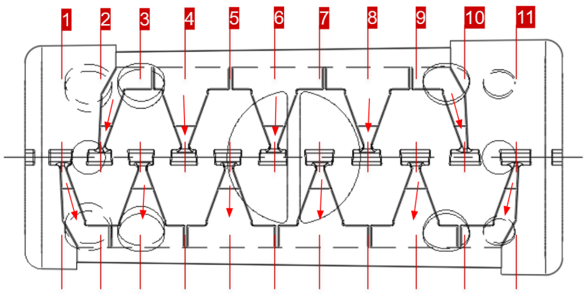

(b)

Figure 6: (a) Cold model of the LINAC-7 project, showing the pick-up ports and tuners and (b) the chosen discretization of the cavity.

5.1. Simulations in ADS

Finally, the specific resonance has been confirmed as the natural mode of the circuit through simulations in ADS (Keysight Technologies, 2024) (Fig. 7).

It is to be noted that the final resonant frequency for this preliminary version of the model (786.15MHz) is very close to the one obtained in the electromagnetic simulations. The mutual inductances, when correctly adjusted, make the TE resonator section of the circuit resonate at the exact same frequency as the cavity without the axis (1.3GHz, obtained in CST by removing the stem and drift tubes from the cavity).

In the bottom part of the Fig. 7 the results of a harmonic balance simulation at the resonant frequency are shown. This allows to check the voltage distribution between consecutive accelerating capacitors C_p, which is the representation of the accelerating field between drift tubes. It can be seen a 180 degree phase shift from one accelerating gap to the other, corresponding to the real behavior of the cavity. The magnitudes are closely related to the voltage distribution of the resonant regions obtained solving 2, but flatter in the middle due to the loading of the axis. This behavior is also observed in the electromagnetic simulations.

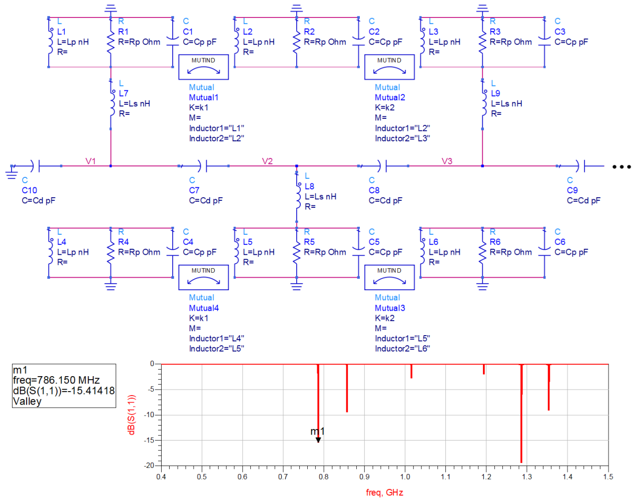

freq	V1	V2	V3	V4	V5	V6
0.0000 Hz 786.1 MHz	0.000 / 0.000 7.494 / -0.475	0.000 / 0.000 13.602 / 179.537	0.000 / 0.000 18.868 / -0.445	0.000 / 0.000 23.469 / 179.581	0.000 / 0.000 26.917 / -0.369	0.000 / 0.000 28.324 / 179.605

Figure 7: Schematic of the circuit in ADS and the S-parameters and Harmonic Balance results for $C_p = 0.12$pF, $L_p = 49$nH, $C_d = 0.13$pF and $L_s = 4$nH. Only the first 6 out of 11 sections' results have been captured as the structure is symmetric. It can be seen that, for the first resonance (786.15MHz) the mode behaves as expected. The results of the table below show the magnitude (in volts) and phase (in degrees) of a harmonic balance simulation at the resonant frequency.

The final challenge in achieving the desired model response involves adjusting these k_i coefficients to match the physical voltage distribution. In order to obtain a first approximation of these parameters correctly, a simplified model has been used where all the C_p, L_p, C_d and L_s parameters are equal. This allows to reduce the number of variables significantly so that a manual adjustment can be carried out. The preliminary results show great agreement with the analytical results and the general behavior is compatible with the electromagnetic simulations. In order to consider the different values of capacitor and inductor and better replicate the behavior of the actual structure, an automated mechanism to tune the mutual inductances must be developed.

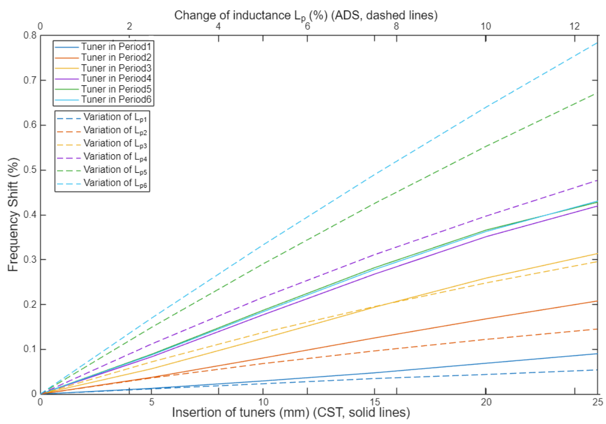

Figure 8: Relationship between tuner insertion (top) and incremental change in inductance (bottom) for each resonator and its corresponding frequency shift induced within the whole cavity.

Once the fundamental circuit behavior has been established, the influence of the tuners can be incorporated into the model. This is a work in progress, but preliminary results in the symmetric circuit show that the voltage distribution obtained with the proposed model is directly linked to the frequency shift caused by varying the inductance L (which represents the tuner effect) in each resonator. Furthermore, the resonant frequency shift exhibits a linear relationship with the inductance variation, mirroring the response observed when changing the tuner penetration depth in the electromagnetic simulations (Fig. 8). The effect on each section could be adjusted by changing the corresponding k_i coefficient, which is a promising result for the future development of the model.

6. Conclusions and future work

This work has presented a methodology to characterize the individual accelerating sections of an IH-DTL cavity as standard electrical components, facilitating their integration into control-oriented simulation frameworks. By developing a distributed equivalent circuit, it has been possible to capture localized spatial dependencies that global analytical models fail to represent, which is a fundamental advancement for modeling the sensitivity of the system to specific actuators such as mechanical tuners. This approach provides a reliable basis for verifying the consistency between full-wave electromagnetic simulations and circuit theory. The proposed model has been applied to the cold model of the LINAC-7 IH-DTL, and the results are promising, showing that the circuit-based approximations align well with the complex electromagnetic behavior of the structure.

Nevertheless, it must be emphasized that this model is not yet the final representation of the whole system and significant work remains to be completed for its application in control environments. First, a systematic method is required to easily adjust the mutual coupling coefficients (k_i) and the resulting voltage distribution curve to optimize the correspondence between the circuit model and the physical cavity response. Finally, future research must characterize the precise effect of the power coupler position on field distribution and expand the model to test power recombination strategies for configurations using multiple couplers, ensuring the synchronization and efficiency required for the control objectives. The modeling of the tuners has been preliminarily included in the model with quite good results, but similar characterizations are lacking for other effects as microphonics, environmental disturbances or manufacturing tolerances. Once the model is fully characterized, it will be possible to use it in control-oriented simulations to test different control strategies and evaluate their performance in terms of stability, robustness, and efficiency. This will be a crucial step towards the development of a reliable and efficient LLRF control system for IH-DTL cavities.

Acknowledgments

This work has been partially supported by the PID2023-148792OB-I00 project funded by MICIU/AEI /10.13039/501100011033 and by FEDER, UE.

References

Dassault Systèmes, 2024. CST Studio Suite. Dassault Systèmes, Darmstadt, Germany, version 2024.01.

Feuchtwanger, J., Etxebarria, V., Portilla, J., Jugo, J., Arredondo, I., Badillo, I., Asua, E., Vallis, N., Elorza, M., Alberdi, B., Enparantza, R., Ariz, I., Muñoz, I., Etxebeste, U., Hernandez, I., 2022. New generation compact linear accelerator for low-current, low-energy multiple applications. Applied Sciences 12 (9).
DOI: 10.3390/app12094118

Ginzton, E. L., 1957. Microwave Measurements. International Series in Pure and Applied Physics. McGraw-Hill, New York, NY.

Grespan, F., De Michele, G., Ramberger, S., Vretenar, M., 2010. Circuital Model for Post Coupler Stabilization in a Drift Tube Linac. Tech. rep., CERN, Geneva.

Jia, X.-Y., Zheng, S.-X., Dec. 2013. Analyzing the effects of post couplers in dtl tuning by the equivalent circuit model. Chinese Physics C 37 (12), 127005.
DOI: 10.1088/1674-1137/37/12/127005

Keysight Technologies, 2024. Advanced Design System (ADS). Keysight Technologies, Santa Rosa, CA, USA, version 2024.

Lu, Y., Ratzinger, U., Schlitt, B., Tiede, R., 2007. The general rf tuning for ih-dtl linear accelerators. Nuclear Instruments and Methods in Physics Research Section A: Accelerators, Spectrometers, Detectors and Associated Equipment 582 (2), 336–344.
DOI: https://doi.org/10.1016/j.nima.2007.08.177

Ratzinger, U., 2005. H-type linac structures. Tech. rep.
DOI: 10.5170/CERN-2005-003.351

Tan, Q., Easton, M., Qi, F., Gan, P., Li, H., Lu, Y., Wang, Z., 05 2018. Multiphysics analysis of a cw ih-dtl for cifnef.
DOI: 10.18429/JACoW-IPAC2018-TUPAL052

Wangler, T. P., 2008. RF Linear Accelerators, 2nd Edition. Wiley-VCH, Weinheim, Germany.
DOI: 10.1002/9783527623426